

## Dispersion of Polyethylene Glycol in Perfluorodecalin for Liquid Phase Fluorination

A.A. Andreev<sup>1\*</sup>, N.A. Belov<sup>1,2</sup>, V.V. Makarova<sup>2</sup>, G.A. Shandryuk<sup>2</sup>, D.V. Bryankin<sup>1</sup>,  
D.S. Pashkevich<sup>1,3</sup>, A.Yu. Alentiev<sup>1,2</sup>

<sup>1</sup>National Research Tomsk Polytechnic University, 30, ave. Lenina, Tomsk, Russia

<sup>2</sup>A.V. Topchiev Institute of Petrochemical Synthesis, Russian Academy of Sciences,  
29, Leninsky ave., Moscow, Russia

<sup>3</sup>Institute of Applied Mathematics and Mechanics, Peter the Great St. Petersburg Polytechnic University,  
29, Polytechnicheskaya, Str. Petersburg, Russia

### Article info

*Received:*

14 April 2022

*Received in revised form:*

7 June 2022

*Accepted:*

23 August 2022

### Keywords:

Polyethylene glycol,  
Perfluorodecalin,  
Liquid-liquid systems,  
Ultrasonic emulsification,  
Bubbling, Coagulation,  
Breakage.

### Abstract

This work aims to obtain the dispersions based on polyethylene glycols (PEGs) of various molecular masses (MM) and perfluorodecalin (PFD) for subsequent direct fluorination. The solubility of the components was estimated using laser interferometry and differential scanning calorimetry, and it was shown that PEGs with different MM are not highly compatible with PFD. The dispersions were prepared during sonication. Gel permeation chromatography (GPC) analysis indicated that MMs almost did not change in this process. While the sonication of PEG-PFD, there is a formation of dispersion with the particle sizes distribution in a range of 0.4–2  $\mu\text{m}$  depending on the MM of PEG. The dispersion is metastable for several hours, even though its stability was significantly affected by additional bubbling with the gas flow. Moreover, the dispersions with a solid PEG phase (MM > 600 Da) were subjected to a smaller change compared to a liquid one (MM < 600 Da). The results of this research shed light on the applicability of the ultrasonic preparation of PEGs in PFD for liquid-phase fluorination with obtaining perfluorinated polyether of target MM.

## 1. Introduction

Perfluorinated polyethers and their derivatives with functional end groups are widely used in chemical synthesis to obtain modern materials due to their unique properties [1, 2]. Thus, materials based on perfluoroethylene glycol (PEG) ethers have excellent viscosity indices and low-temperature properties, very low evaporative losses, and sufficient thermal stability. These properties make them attractive candidates for low-temperature lubricants [3–7]. Perfluoropolyethers are now considered to be a promising alternative to hydrofluorocarbons because of their low atmospheric lifetimes [8–17].

By now, there are two strategies to obtain perfluoropolyethers – the monomeric pathway and direct fluorination. The first one involves the polymerization of perfluorinated monomers and is suffering from the complexity of the structure and properties control of the products obtained, and the inevitability of the formation of residual peroxide groups [15], which upon reduction leads to a decrease in the molecular masses (MM) of oligomers. At the same time, direct fluorination of commercially available polymers using gaseous fluorine is getting more widespread [18–23].

Liquid-phase fluorination provides a reduction in local heat generation during exothermic processes and can be carried out at a higher rate. Liquid-phase fluorination is performed by dissolving the starting substance, or otherwise, suspensions and emulsions are fluorinated.

\*Corresponding author.

E-mail addresses: andreevaa@tpu.ru

It has been shown that fluorination of PEG solutions is taking place without the carbon backbone of the polymer changing [22, 24], but the use of expensive, toxic, ozone-depleting liquids as the liquid phase [25–27] limits its industrial applications.

Fluorination of polymers in a perfluorinated liquid medium, such as perfluorodecalin (PFD), is a promising method to obtain fluorinated polymers [28–30] due to the high chemical resistance of perfluorocarbons and the solubility of gases in them. It was shown in [28] that surface fluorination is accompanied by the dissolution of a fluorinated polymer in PFD, which means that providing a high interface for liquid-phase fluorination in PFD significantly affects the rate of the process.

This work investigates a system of PEG and PFD for subsequent fluorination. In this study, there is a demonstration of the compatibility of PEGs and PFD, as well as the determination of the sonication aspects that contribute to obtaining the emulsions of PEGs in PFD. There is also a discussion of the sonication effect on the changes in the molecular mass distribution of PEGs with different molecular masses. The research results will make it possible to establish the feasibility and determine the parameters of fluorination of PEGs in PFD to obtain perfluoropolyethers with target MM.

## 2. Materials and Methods

### 2.1. Materials

PFD with the main substance content of 99.2%, and PEG with MM of 200, 300, 400, 600, 1500, 4000, 6000, 10000 were purchased from Fluorine Salts Chemical Plant LLC. Additionally, PEG with MM of 40000 Da was obtained from Forward Group LLC. Chloroform of spectrophotometric grade for gel permeation chromatography (GPC) analysis was obtained from Sigma Aldrich.

For GPC system calibration InfinityLab EasiVial PEG/PEO standards (Agilent Technologies) were used.

### 2.2. Laser interferometry

The compatibility of PFD with PEGs was studied by laser interferometry [31, 32]. For that, PEG was placed between the two glass slides with a gap thickness of 60  $\mu\text{m}$  controlled by the spacers. In the case of solid PEG, the diffusion cell was formed at a temperature of 60  $^{\circ}\text{C}$ . Then PFD was poured into the cells. The moment of contact of

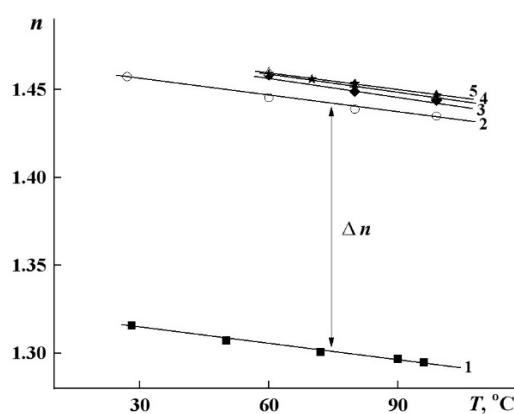


Fig. 1. Thermal dependences of refractive indices for PFD (1), PEG 300 (2), PEG 1500 (3), PEG 10000 (4) and PEG 40000 (5).

the components was an indicator of the beginning of the diffusion process. The measurements were carried out in the mode of a stepwise increase and decrease of temperature from 20 to 120  $^{\circ}\text{C}$ . A modular KLM-A532-15-5 laser with a wavelength of 532 nm was used as a light source. The interference patterns were recorded using a digital camera with the image transferred to PC.

Thermal dependences of individual components refractive indexes were previously determined using refractometry (Fig. 1). The measurements were carried out with the refractometer IRF-22 connected to the Huber CC304 thermostat. For all the components, linear dependencies were observed. The differences in refractive indices between PFD and PEGs were 0.14–0.15, which corresponds to the formation of 32–35 interference bands in the diffusion zone.

### 2.3. Differential scanning calorimetry

The preparation of PEG and PFD mixtures was carried out directly in crucibles. For this purpose, the required amounts were placed in a crucible located on the balance (Mettler Toledo XPR205) with an accuracy of 0.01 mg. In general, the total weight of each mixture was about 10 mg, but for every case, it was weight with a high accuracy for future calculations. Then the crucible was hermetically sealed to ensure a constant composition of the mixture in the entire temperature range of measurements.

A homogeneous mixture was forming after 20 min at a temperature 30  $^{\circ}\text{C}$  above the melting point of the most high-melting component. Then the mixture was cooled down to the temperature 30  $^{\circ}\text{C}$  below the phase transition temperature of

the most low-melting component at the rate of 10 °C/min and was held at this point for 10 min. After that, the final heating at a rate of 10 °C/min was done. Schematically, the procedure of this heat treatment is shown in Fig. S1. The melting points and enthalpies of fusion for the initial crystalline PEGs were calculated based on the results of the second heating.

#### 2.4. The dispersion formation by sonication

PEG dispersion was carried out using the ultrasonic disperser UZDN-0.3 manufactured by Kriamid LLC (Moscow, Russia). The unit consists of the following components: ultrasonic generator GU-22-800 with a maximum power of 800 W, adjustable pulse voltage from 200 to 500 V, and frequency from 22 to 23 kHz to adjust the resonance of the system; oscillation system, representing an assembly of the magnetostrictive transducer with water cooling; and submersible titanium acoustic waveguide with a diameter of 5 mm.

PEGs and PFD weights of the required ratio were placed into a 50 ml glass beaker, then the acoustic waveguide of the ultrasonic dispersant was immersed into 2–5 mm of the initial reagents layer. After that, the dispersant was turned on, and the frequency was adjusted to the resonance of the system for maximum cavitation in the reaction volume. The ultrasonic treatment time was 3 min. In the case of GPC experiments, the treatment time was prolonged to 45 min. The samples of high molecular mass PEGs were preheated until they were completely melted in PFD. Melting points for PEGs with MM of 600, 1500, 4000, 6000 Da were equal to 30 °C, 52.3 °C, 65.6 °C, and 73.1 °C, respectively, according to TGA-DSC analysis.

Due to the sonication, the temperature of 25 ml emulsion increased from 20 to 80 °C in 30 min.

#### 2.5. Gravimetric method to determine the concentration of PEG emulsions in PFD

It was experimentally confirmed that the evaporation rates of PEGs are 100–1000 times lower than that of PFD at temperatures of 50–140 °C (Table 1). The gravimetric method is required to determine the mass of PEG in the emulsion, taking into account that at a given temperature, all PFD volume will evaporate, and all PEG will remain in a condensed state. For this purpose, crucibles with emulsion weights of about 20 g were placed in a drying cabinet, which provided a stable tempera-

**Table 1**  
Evaporation rates of PEGs and PFD  
at different temperatures

Substance	Evaporation rates, mg/min		
	50 °C	100 °C	140 °C
PFD	200	244	480
PEG200	0.35	0.57	4.78
PEG400	0.11	0.13	0.4
PEG600	0.09	0.1	0.3
PEG1500	0.1	0.11	0.22
PEG4000	0.1	0.12	0.27
PEG6000	0.1	0.11	0.24

ture control mode. The mass measurements were carried out using an Acculab ALC-210d4 analytical balance.

#### 2.6. Particle size determination

To estimate the emulsified PEGs particle sizes in the obtained suspensions (emulsions), the particle size analyzer DelsaMax Pro (Beckman Coulter) was used. The dispersity was measured at the 589 nm wavelength; the thermostat temperature of the measuring cell was 21 °C. To evaluate the error bar, there were 10 dispersity measurements with a duration of 5 s. The procedure was repeated 5 times for each sample. In the end, an aliquot was taken from the volume of the emulsion and put into a dry purified polymer 1.5 ml cuvette.

The average radius of particles was measured 0.5–6 hours after ultrasonic exposure of the emulsions of PFD and PEGs with MM of 200, 400, 600, 1500, 4000, 6000. The average radius of particles after bubbling with a duration from 0 to 40 min was also determined. The bubbling was carried out through a layer of emulsion placed into a 10 ml tube made of HANNA borosilicate glass. To do this, the air was supplied with a flow rate of 5 L/hour through a siphon lowered to the bottom of the tube.

#### 2.7. Gel permeation chromatography

The GPC LC-20 Prominence (Shimadzu, Japan) system consists of a LC-20 AD HPLC pump (Shimadzu, Japan), DGU-203R Prominence Degasser (Shimadzu, Japan), CTO-20A/AC column oven (Shimadzu, Japan), RID-20A (Shimadzu, Japan) refractive index detector and 7.5×300 mm Agilent Technologies column (PLgel 5 µm

MIXED-C, providing an effective molecular mass range of 200 to  $4 \times 10^5$  Da). The volume of injection was 20  $\mu\text{L}$ . Chloroform with a flow rate of 1 mL/min at 40 °C was used as an eluent.

The samples of the original PEGs as well as reference samples were dissolved in chloroform before the analysis. In the case of the PEGs study, after sonication PFD was first evaporated from the emulsion under a vacuum at 60 °C, and the residue was dissolved in chloroform. Before the analysis, all the samples were filtered through PTFE filters with a pore size of 0.75  $\mu\text{m}$ .

The GPC system was calibrated with PEG standards in the molecular mass range from 194 to 34520 g/mol (regression equation of the calibration curve is  $y = 32986 \cdot x - 8.22$ ;  $R^2 = 0.9998$ , where  $x$  – time, min;  $y$  – LogMM). Weight ( $M_w$ ) and number ( $M_n$ ) of average molecular masses were evaluated using Shimadzu LC Solution software. The polydispersity index (PDI) was calculated as the ratio between  $M_w$  and  $M_n$ .

### 3. Results and discussion

#### 3.1. Compatibility of PEG-PFD

Figure 2 shows typical interferograms of the interdiffusion zones formed in the contact of PEG and PFD phases. The interference bands on both sides of the interface did not change at any temperature regardless of the molecular mass from the molecular mass of PEG. These results indicate that there is no penetration of the components into each other, and show the incompatibility of PFD with PEG.

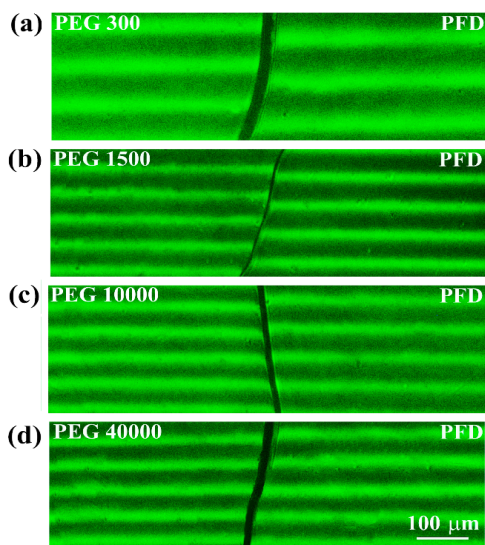


Fig. 2. Interferograms of the PEG-PFD systems at (a) – 54 °C, (b) – 70 °C, (c) – 110 °C and (d) – 60 °C.

The phase transitions of the individual components were observed for all of the studied PEG–PFD compositions (Fig. S2.A–C). However, there are minor shifts in the temperature transitions. The drop in phase transition temperatures with an increase in PEG concentration according to DSC data can be explained by the cryoscopic effect. However, in this case, the components are not able to form a homogeneous solution in the liquid phase and are separated due to high differences in density. In addition, there is a decrease in the heat of the PFD phase transition (compared to the expected value based on the loading of the components), which is usually about 1% of the normalized value. At the same time, the enthalpies of fusion of the PEG1500 and PEG40000 crystalline phases remain close to the expected value. Unlike the others, in a mixture with PFD, PEG300 significantly loses a fraction of the crystallizing phase (Fig. S2.A), however, it initially tends to overcooling and, in the case of the shortest chain, has a defective crystal structure.

The PEG1500-PFD system was studied in more detail. The dependences of the temperature changes of the PEG1500 and PFD phase transitions are shown in Fig. 3. The effect of the change in  $T_{mp}$  for the entire phase diagram (Fig. 3) fits in an interval of 1 degree, which indicates extremely low compatibility of the components in the isotropic phase.

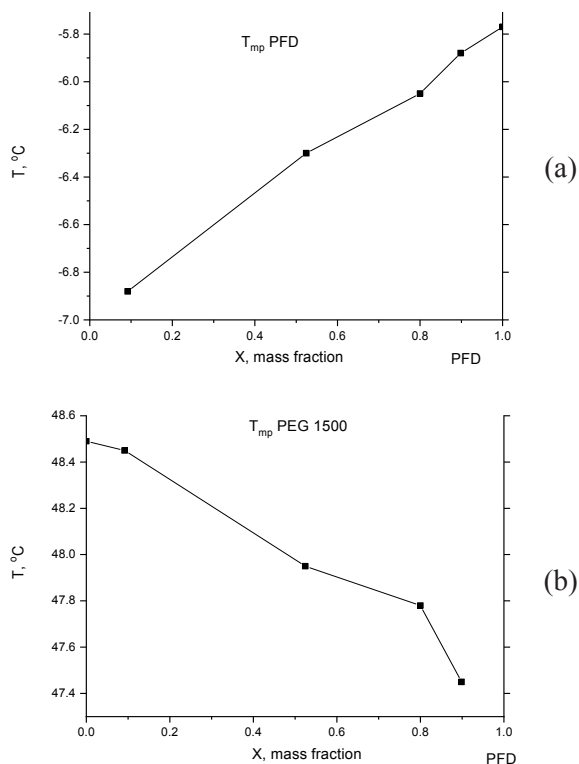


Fig. 3. PFD (a) and PEG1500 (b) melting points ( $T_{mp}$ ) in PEG1500-PFD systems.

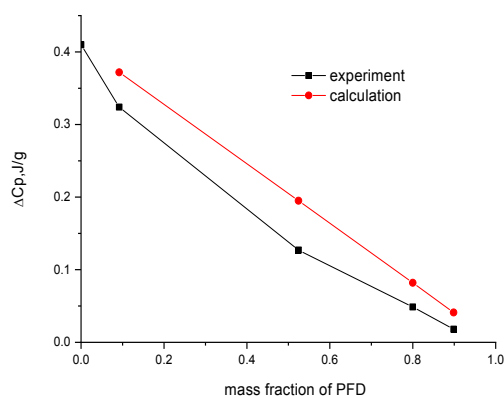


Fig. 4. PEG1500 heat capacity at  $T_g$  range in the PEG1500-PFD systems.

Figure 4 shows the correlation between the calculated and experimental data (Fig. 2C) on the change in heat capacity ( $\Delta C_p$ ) for the PEG1500-PFD system in the glass transition ( $T_g$ ) range. At the same time, it was found that  $T_g$  remains in the same range, although the magnitude of the jump in heat capacity is slightly less than the expected value. This fact can be associated with the cryoscopic effect when the accessibility for interaction increases in comparison with the densely packed crystalline phase. However, this effect is negligible.

### 3.2. Effect of PEG-PFD dispersion sonication on MM of PEG

Due to the close to none solubility of PEG in PFD, it was decided to investigate the process of dispersion of PEG in PFD using an ultrasonic dispersant. It is known [33, 34] that ultrasonic treatment may lead to a change in the molecular mass distribution (MMD) of polymers, which could critically change the structure and properties of the resulting product. In this regard, we conducted a study of PEGs MMD before and after sonication using the GPC method. The optimal sonication time of 3 min was determined experimentally. The fluorination processes may occur within a few hours, which indicates the potential need for periodic ultrasonic treatment to maintain a high surface area of the PEG-PFD interface. In this regard, the sonication time was increased 15 times to conduct GPC analysis.  $M_w$  and  $M_n$  average MM as well as PDI as a measure of molecular mass distribution are shown in Table 2 and Figs. S3.A-F.

As one can see, the  $M_w$ ,  $M_n$  and PDI of the original PEGs and PEGs after sonication are not that different. It means that the selected dispersion mode does not affect the structure of the initial polymer significantly, which helps to predict the

**Table 2**  
 $M_w$ ,  $M_n$  and PDI before and after ultrasonic treatment

Substance	Before ultrasonic			After ultrasonic		
	$M_n$ , Da	$M_w$ , Da	PDI	$M_n$ , Da	$M_w$ , Da	PDI
PEG200	180	206	1.44	175	190	1.09
PEG400	333	405	1.22	342	419	1.23
PEG600	496	600	1.21	514	610	1.19
PEG1500	919	1330	1.44	929	1918	1.42
PEG4000	2203	3633	1.65	2261	3567	1.58
PEG6000	4952	5565	1.21	4402	5651	1.28

molecular mass of the final product with greater accuracy. Also, the selected dispersion mode can be used during the fluorination process to maintain a high interface area in the PEG-PFD system.

### 3.3. Investigation of PEG dispersions in PFD after sonication

Most of PEG is getting separated from PFD within 30 min after the termination of the ultrasonic dispersion as was shown with the measurements. After 30 min, PFD contains about 0.1 wt.% of the dispersed PEG. The characteristic breakdown time of this dispersion is tens and hundreds of hours. Thus, this system was proposed to be called a metastable dispersion.

Table 3 shows the concentrations of PEGs with different molecular masses in a metastable dispersion 1 h after the termination of sonication, according to gravimetric method data.

Based on the studies to determine the concentration of PEG in the emulsions, the concentration of PEG in the emulsions depends on the molecular mass of PEG and the time passed after sonication. A decrease in the molecular mass of PEG from 6000 to 200 Da leads to an increase in concentration from 0.08 to 0.7 wt.%.

**Table 3**  
Concentrations of PEGs in metastable emulsions of PEG-PFD

Substance	Concentration of PEG in the emulsion, %	Concentration of PEG in the emulsion, g/L
PEG200	0.6-0.7	3.1-3.6
PEG400	0.25-0.3	1.4-1.55
PEG600	0.1-0.13	0.6-0.68
PEG1500	0.09-0.13	0.48-0.69
PEG4000	0.08-0.09	0.3-0.4
PEG6000	0.08-0.09	0.3-0.38

To increase the concentration of emulsified PEG in PFD, it is required to take the shortest possible time from sonication to the beginning of fluorination.

The concentration of PEG in a metastable dispersion decreases over time by  $5\pm 1\%$  per hour in the range from 1 to 6 h after dispersion, while the rate of concentration change does not depend either on the molecular mass of PEG or on the temperature values.

Figure 5 demonstrates the dependence of the radius of PEG particles in PFD on the dispersion hold time. After 30 min from the end of ultrasonic treatment, the characteristic radius of the particles is equal to 200–500 nm, while after 6 h it increases to 600–950 nm. 2 hours after sonication the radius of the PEG particles increases by  $50\pm 10$  nm/h for low molecular mass PEGs (PEG200, PEG 400, PEG600) and by  $25\pm 5$  nm/h for high molecular mass PEGs (PEG1500, PEG 4000, PEG6000) at 21 °C.

To determine the effect of dispersion mixing and the presence of a gas phase in it on the rate of particle size increase, there was a nitrogen stream introduction into the dispersion. Figure 6 shows the dependence of the average radius of PEGs with different molecular masses particles at the time of the process. During 40 min of bubbling, the characteristic radius of the particles increased from 200–500 to 1500–4000 nm.

The average radius of PEG particles increased by  $40\pm 4$  nm/min for PEG200 and PEG400,  $20\pm 4$  nm/min for PEG600,  $145\pm 10$  nm/min for PEG1500,  $125\pm 10$  nm/min for PEG4000, and  $105\pm 10$  nm/min for PEG6000 after 20 min from the start of bubbling. The greater stability of the emulsion is observed for PEGs with MM of 600–6000, which

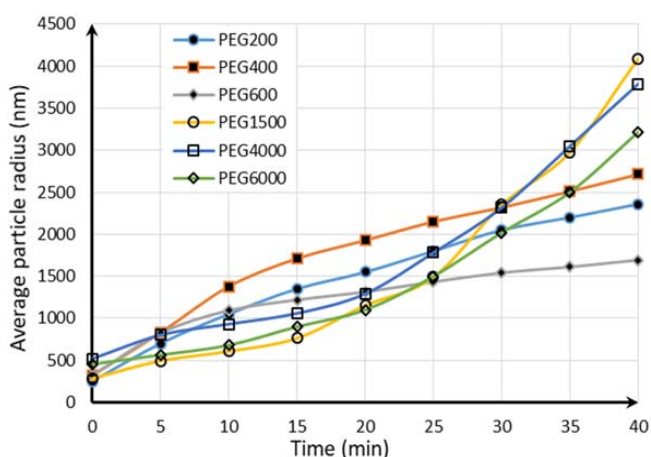


Fig. 6. PEG average particle radius in the emulsions over time (with bubbling).

could be explained by the solid state of PEG in these dispersions.

Since the fluorination of PEG in the investigated system is the surface process, fluorination under mild conditions requires maintaining the size of the emulsified PEG particles at an optimal level. Taking into account the depth of surface fluorination of polymers, which is about 0.1–10  $\mu\text{m}$  [21], the optimal average radius of PEG particles should not be exceeded.

## 4. Conclusions

Laser microinterferometry and DSC methods showed that PEGs of various molecular masses are interinsoluble, which justified the need for ultrasonic dispersion. The effect of sonication on the chemical structure of the dispersed PEGs of various MMs was tested in separate experiments, and no significant changes were found.

The concentrations of PEG in the emulsions with PFD were gravimetrically determined for PEGs of various molecular masses, as well as over time, and the change in PEG concentrations in metastable emulsions was shown. The average concentration of PEG in a metastable emulsion with PFD was 0.08–0.7 wt.%. The average radius of PEG particles in the emulsions increased depending on the aging time of the dispersion. Particle size growth acceleration was observed for gas bubbling.

Since ultrasonic emulsification is not accompanied by a change in MM of PEGs, ultrasonic emulsification of PEG in PFD allows one to obtain and, if necessary, maintain the size of PEG particles and the interface area at an optimal level, which is useful to predict MM of perfluoropolyether upon liquid-phase fluorination of PEG in PFD.

Altogether, the results of the conducted studies allow one to conclude that it is advisable to carry out liquid-phase fluorination of PEGs of various MM using ultrasonic emulsification in PFD.

## Funding

This research was funded by Ministry of Science and Higher Education of Russian Federation, project FSWW-2020-0020.

## Appendix A. Supplementary data

Supplementary data related to this article can be found at <https://doi.org/10.18321/ectj1439>.

## References

- [1]. Z. Hu, J.A. Finlay, L. Chen, D.E. Betts, et al., *Macromolecules* 42 (2009) 6999–7007. DOI: [10.1021/ma901227k](https://doi.org/10.1021/ma901227k)
- [2]. F. Martini, R. Biancardi, E. Barchiesi, S. Borsacchi, et al., *J. Fluorine Chem.* 192 (2016) 22–26. DOI: [10.1016/j.jfluchem.2016.10.006](https://doi.org/10.1016/j.jfluchem.2016.10.006)
- [3]. K. Johns, C. Corti, L. Montagna, P. Srinivasan, *J. Phys. D Appl. Phys.* 25 (1992) A141–A146. DOI: [10.1088/0022-3727/25/1A/022](https://doi.org/10.1088/0022-3727/25/1A/022)
- [4]. G. Marchionni, M. Avataneo, U. De Patta, P. Maccone, et al., *J. Fluorine Chem.* 126 (2005) 463–471. DOI: [10.1016/j.jfluchem.2004.10.048](https://doi.org/10.1016/j.jfluchem.2004.10.048)
- [5]. G. Marchionni, P. Maccone, G. Pezzin, *J. Fluorine Chem.* 118 (2002) 149–155. DOI: [10.1016/S0022-1139\(02\)00226-9](https://doi.org/10.1016/S0022-1139(02)00226-9)
- [6]. G. Marchionni, S. Petricci, P.A. Guarda, G. Spataro, et al., *J. Fluorine Chem.* 125 (2004) 1081–1086. DOI: [10.1016/j.jfluchem.2004.01.027](https://doi.org/10.1016/j.jfluchem.2004.01.027)
- [7]. T. Kaldoński, P.P. Wojdyna, *J. KONES Powertrain Transp.* 18 (2011) 163–184.
- [8]. L.P. Viegas, *J. Phys. Chem. A* 125 (2021) 4499–4512. DOI: [10.1021/acs.jpca.1c00683](https://doi.org/10.1021/acs.jpca.1c00683)
- [9]. L.P. Viegas, *J. Phys. Chem. A* 122 (2018) 9721–9732. DOI: [10.1021/acs.jpca.8b08970](https://doi.org/10.1021/acs.jpca.8b08970)
- [10]. G. Marchionni, P.A. Guarda, U.S. Patent, Process for preparing peroxidic perfluoropolyoxyalkylenes. Patent number 5744651. Date of Patent Apr. 28, 1998.
- [11]. G. Marchionni, M. Visca, European Patent Application, Perfluoropolyethers (PFPEs) having at least an alkylether end group and respective preparation process, EP 1275678A2, January 15, 2003
- [12]. M.P. Sulbaek Andersen, M.D. Hurley, T.J. Wallington, F. Blandini, et al., *J. Phys. Chem. A* 108 (2004) 1964–1972. DOI: [10.1021/jp036615a](https://doi.org/10.1021/jp036615a)
- [13]. W. Navarrini, M. Galimberti, G. Fontana, U.S. Patent, Process for preparing hydrofluoroethers. Patent No.: 7141704B2, Date of Patent: 28 Nov. 28, 2006.
- [14]. M. Wu, W. Navarrini, M. Avataneo, F. Venturini, M. Sansotera, M. Gola, *Chemistry Today* 29 (2011) 67–71.
- [15]. M. Wu, W. Navarrini, G. Spataro, F. Venturini, et al., *Appl. Sci.* 2 (2012) 351–367. DOI: [10.3390/app2020351](https://doi.org/10.3390/app2020351)
- [16]. L.P. Viegas, *Int. J. Chem. Kinet.* 51 (2019) 358–366. DOI: [10.1002/kin.21259](https://doi.org/10.1002/kin.21259)
- [17]. L.P. Viegas, *Theor. Chem. Acc.* 138 (2019) 65. DOI: [10.1007/s00214-019-2436-z](https://doi.org/10.1007/s00214-019-2436-z)
- [18]. J.A.C. Allison, G.H. Cady, *J. Am. Chem. Soc.* 81 (1959) 1089–1091. DOI: [10.1021/ja01514a018](https://doi.org/10.1021/ja01514a018)
- [19]. A.P. Kharitonov, G.V. Simbirtseva, V.M. Bouznik, M.G. Chepezubov, et al., *J. Polym. Sci. Pol. Chem.* 49 (2011) 3559–3573. DOI: [10.1002/pola.24793](https://doi.org/10.1002/pola.24793)
- [20]. A.P. Kharitonov, L.N. Kharitonova, *Pure Appl. Chem.* 81 (2009) 451–471. DOI: [10.1351/PAC-CON-08-06-02](https://doi.org/10.1351/PAC-CON-08-06-02)
- [21]. A.P. Kharitonov, *Prog. Org. Coat.* 61 (2008) 192–204. DOI: [10.1016/j.porgcoat.2007.09.027](https://doi.org/10.1016/j.porgcoat.2007.09.027)
- [22]. T. Okazoe, *J. Fluorine Chem.* 174 (2015) 120–131. DOI: [10.1016/j.jfluchem.2014.09.020](https://doi.org/10.1016/j.jfluchem.2014.09.020)
- [23]. N.A. Belov, A.Y. Alentiev, Y.G. Bogdanova, A.Y. Vdovichenko, et al., *Polymers* 12 (2020) 28–36. DOI: [10.3390/polym12122836](https://doi.org/10.3390/polym12122836)
- [24]. T.R. Bierschenk, T.J. Juhlke, H. Kawa, R.J. Lagow, U.S. Patent, Liquid-phase fluorination. Patent number 5753776A, Date of patent: May 19, 1998.
- [25]. R.L. Powell, J.H. Steven, CFCs and the Environment: Further Observations, in: R.E. Banks, B.E. Smart, J.C. Tatlow (Eds.), *Organofluorine Chemistry*, Springer US, Boston, MA, 1994. P. 617–629. DOI: [10.1007/978-1-4899-1202-2\\_31](https://doi.org/10.1007/978-1-4899-1202-2_31)
- [26]. M.B. Blanco, C. Rivala, M.A. Teruel, *Chem. Phys. Lett.* 578 (2013) 33–37. DOI: [10.1016/j.cplett.2013.06.004](https://doi.org/10.1016/j.cplett.2013.06.004)
- [27]. A. Mellouki, T.J. Wallington, J. Chen, *Chem. Rev.* 115 (2015) 3984–4014. DOI: [10.1021/cr500549n](https://doi.org/10.1021/cr500549n)
- [28]. I.A. Blinov, D.A. Mukhortov, Y.P. Yampolskii, N.A. Belov, et al., *J. Fluorine Chem.* 234 (2020) 109526. DOI: [10.1016/j.jfluchem.2020.109526](https://doi.org/10.1016/j.jfluchem.2020.109526)
- [29]. N.A. Belov, I.A. Blinov, A.Yu. Alentiev, V.M. Belokhvostov, et al., *J. Polym. Res.* 27 (2020) 290. DOI: [10.1007/s10965-020-02261-8](https://doi.org/10.1007/s10965-020-02261-8)
- [30]. I.A. Blinov, N.A. Belov, A.V. Suvorov, S.V. Chirkov, et al., *J. Fluorine Chem.* 246 (2021) 109777. DOI: [10.1016/j.jfluchem.2021.109777](https://doi.org/10.1016/j.jfluchem.2021.109777)
- [31]. V. Makarova, V. Kulichikhi, Application of Interferometry to Analysis of Polymer-Polymer and Polymer-Solvent Interactions, in: I. Padron (Ed.), *Interferometry - Research and Applications in Science and Technology*, InTech, 2012. DOI: [10.5772/35816](https://doi.org/10.5772/35816)
- [32]. A.E. Chalykh, U.V. Nikulova, A.A. Shcherbina, E.V. Chernikova, *Polym. Sci. Ser. A* 61 (2019) 175–185. DOI: [10.1134/S0965545X19020020](https://doi.org/10.1134/S0965545X19020020)
- [33]. H. Kawasaki, Y. Takeda, R. Arakawa, *Anal. Chem.* 79 (2007) 4182–4187. DOI: [10.1021/ac062304v](https://doi.org/10.1021/ac062304v)
- [34]. G. Madras, V. Karmore, *Polym. Int.* 50 (2001) 683–687. DOI: [10.1002/pi.677](https://doi.org/10.1002/pi.677)